MRI-driven disk winds and dispersal of protoplanetary disks

Takeru Suzuki
(School of Arts & Sciences, U. Tokyo)

In collaboration with
Shu-ichiro Inutsuka (Physics dept., Nagoya U.)
Takayuki, Muto (Physics dept. Kyoto U.)

Dispersal of Protoplanetary Disks

Current Understandings

Shu et al.1993; Matsuyama et al.2003; Alexander et al.2006 _

- **Outer Region**
  - Evaporation by UV(accretion/chromosphere)

    Uncertainties in UV flux

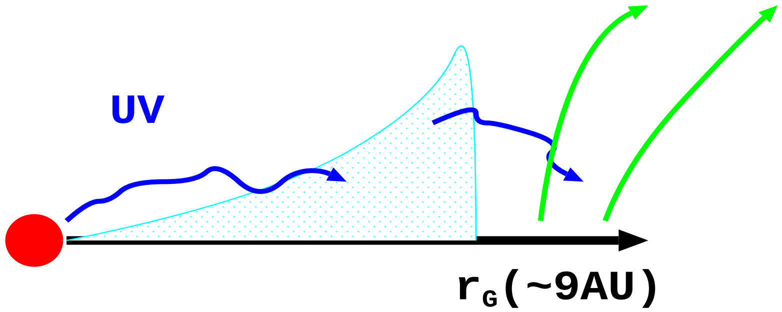

- **Inner Region**
  - Accretion by turbulent viscosity

    Need fundamental properties of turbulence
- **Stellar Winds**
  - Minor Contributions

This Work : Turbulent-driven winds

Disk Winds

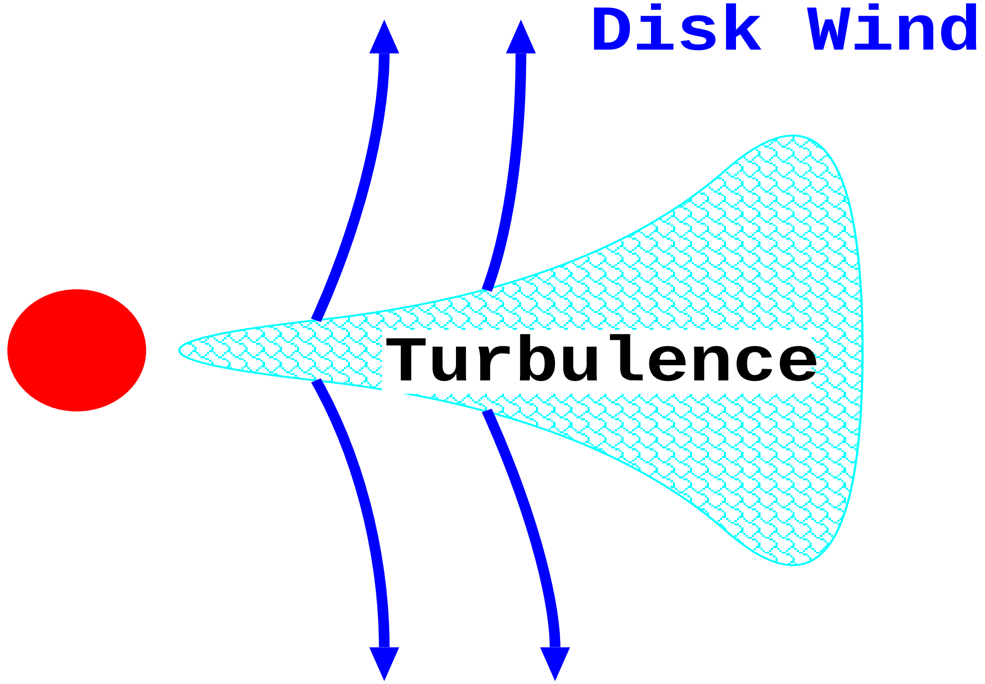

Winds driven by magneto-turbulent pressure

- **MRI triggers the generation of MHD turbulence**
  - **Parker instability also plays a role**

Outline

Evolution of Gas Component of Protoplanetary Disks with Disk Winds

1. Local 3D MHD simulations
   - MHD turbulence => Accretion & Disk Winds

2. Global 1D calculation
   - Results of Local Simulation => Global Evolution

1. Local 3D MHD Simulations

Local Disk Simulations

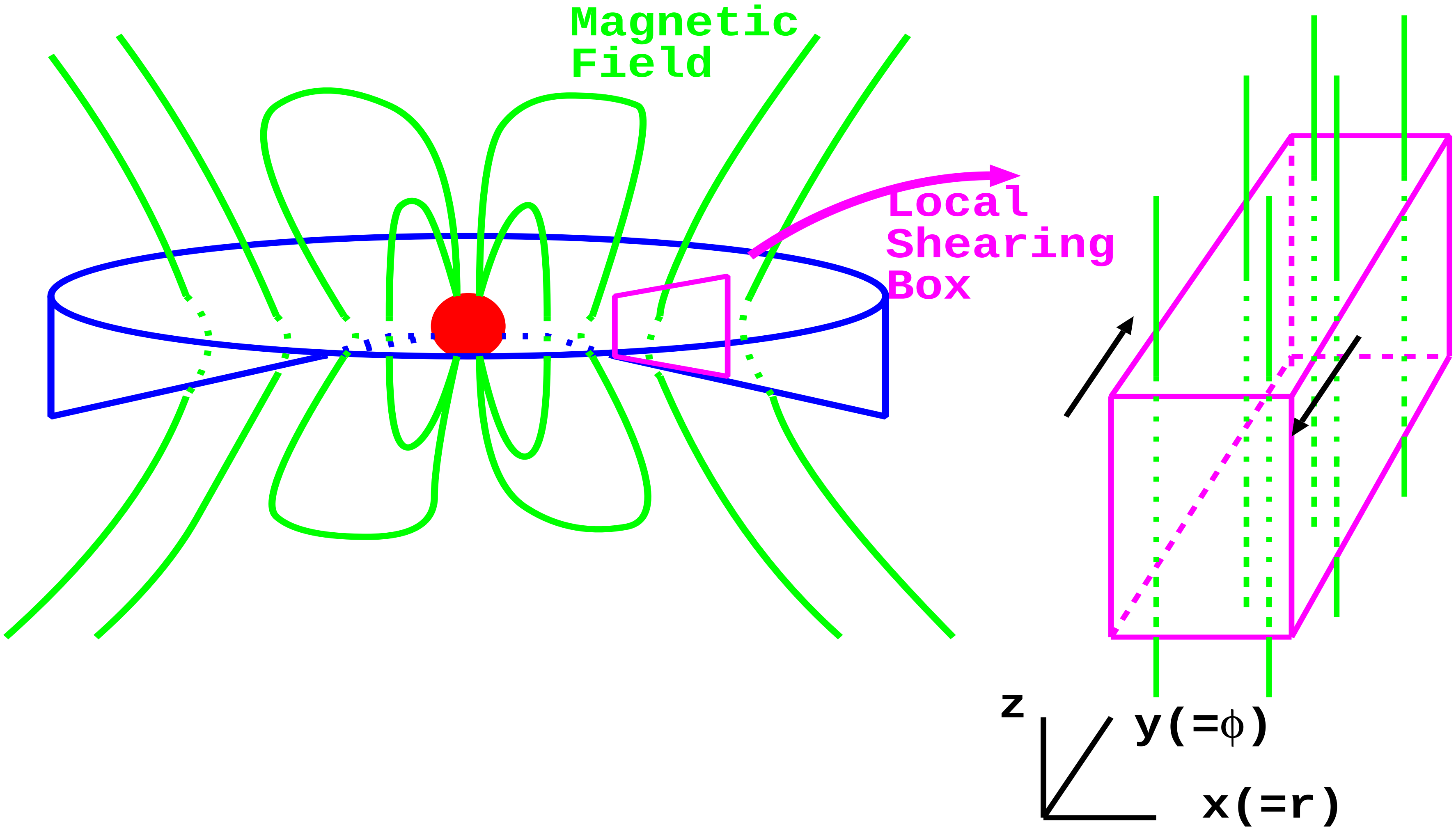

- Local shearing box to mimic differential rotation
  - to resolve fine-scale turbulence

Set-up

- Simulation Box : $-0.5H < x < 0.5H, -2H < y < 2H, -4H < z < 4H$
  $(N_x, N_y, N_z) = (32, 64, 256)\&(64, 128, 512) \qquad H^2 = 2c_s^2/\Omega_0^2$
- Boundaries : shearing in x, periodic in y, & outgoing in z directions
  - Outgoing boundary condition $\neq$ 0-gradient condition
- Initial Conditions
  - Hydrostatic Density : $\rho = \rho_0 \exp(-z^2/H^2)$
  - Kepler Rotation : $v_{y,0} = -(3/2)\Omega_0 x$
  - B-field : $B_{z,0}$ =const or $B_{y,0}$ =const ($\beta_0 \equiv 8\pi\rho_0 c_s^2/B_0^2 = 10^4 - 10^7$)
    - Reference case : net B_z with $\beta_0 = 10^6$ at the midplane.
  - Small v-perturbations : $\delta v = 0.005 c_s$
- Equation
  - both ideal and resistive MHD
  - neglect dusts
  - Isothermal Equation of State

Snapshot Data (t = 0)

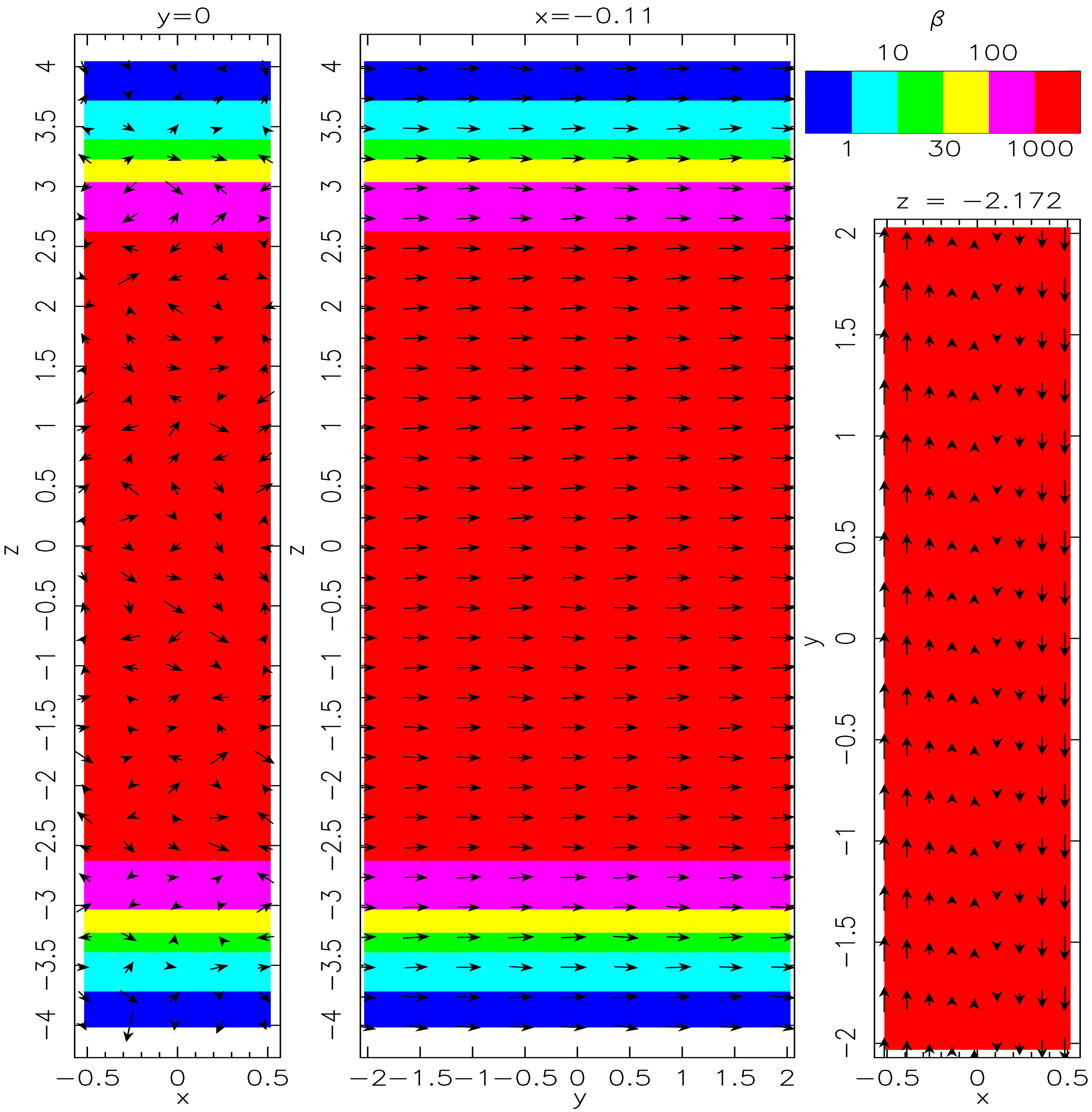

- $\beta = 8\pi\rho c_s^2/B^2$
- Arrows : $\vec{v}$ field

Snapshot Data (t = 10 rot)

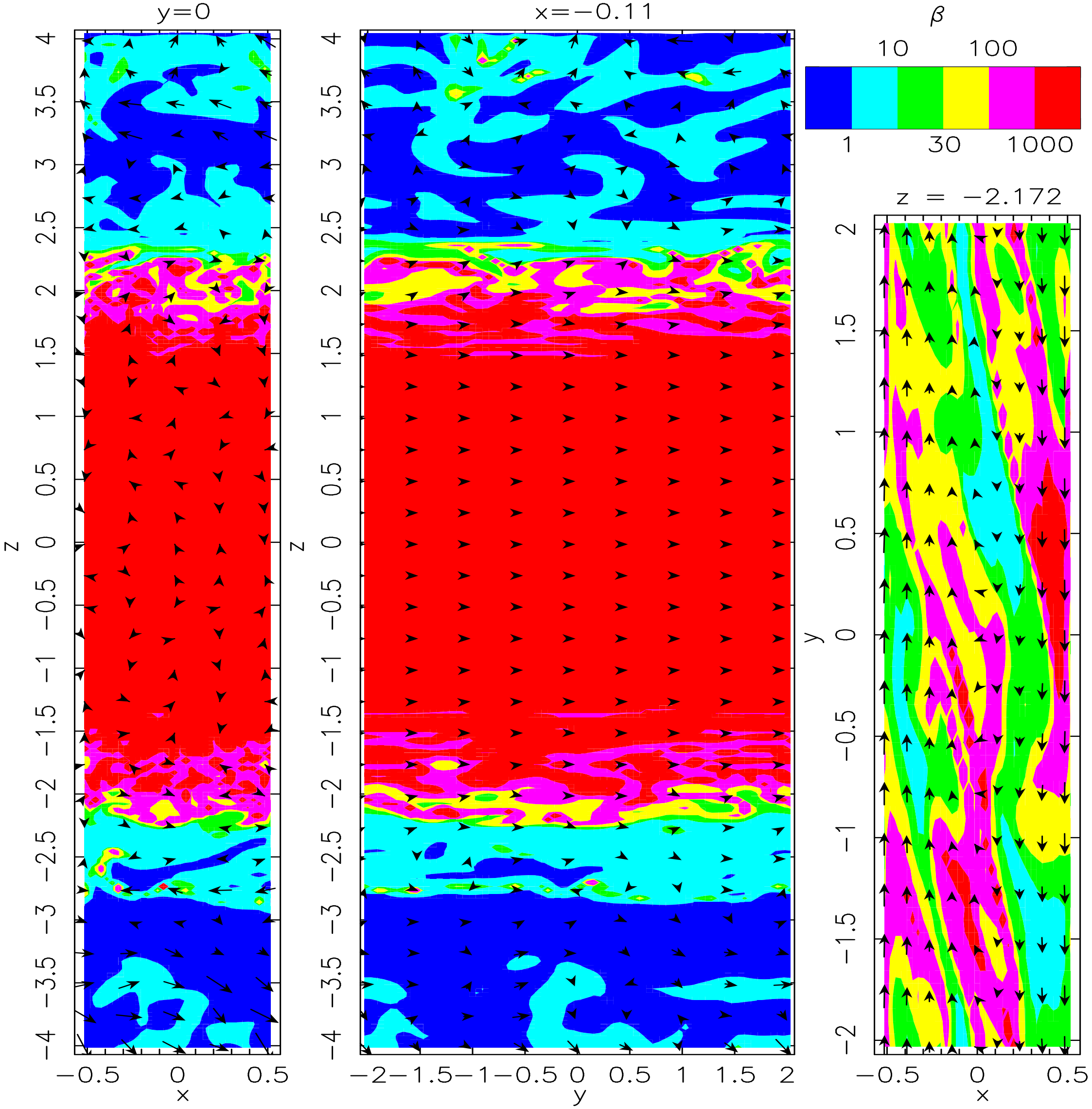

- $\beta = 8\pi\rho c_s^2/B^2$
- Arrows : $\vec{v}$ field

Snapshot Data (t = 50 rot)

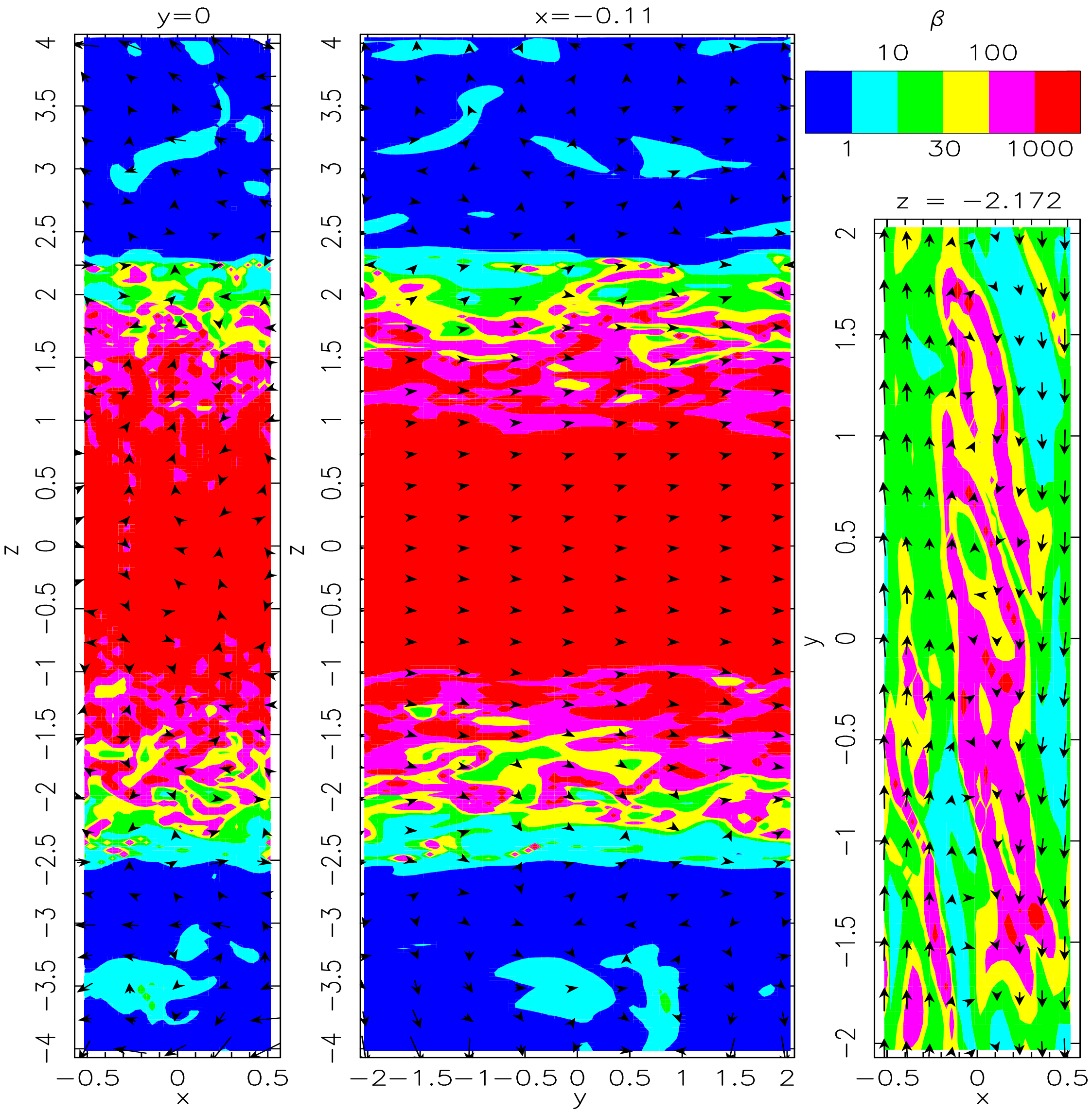

- $\beta = 8\pi\rho c_s^2/B^2$
- Arrows : $\vec{v}$ field

Snapshot Data (t = 100 rot)

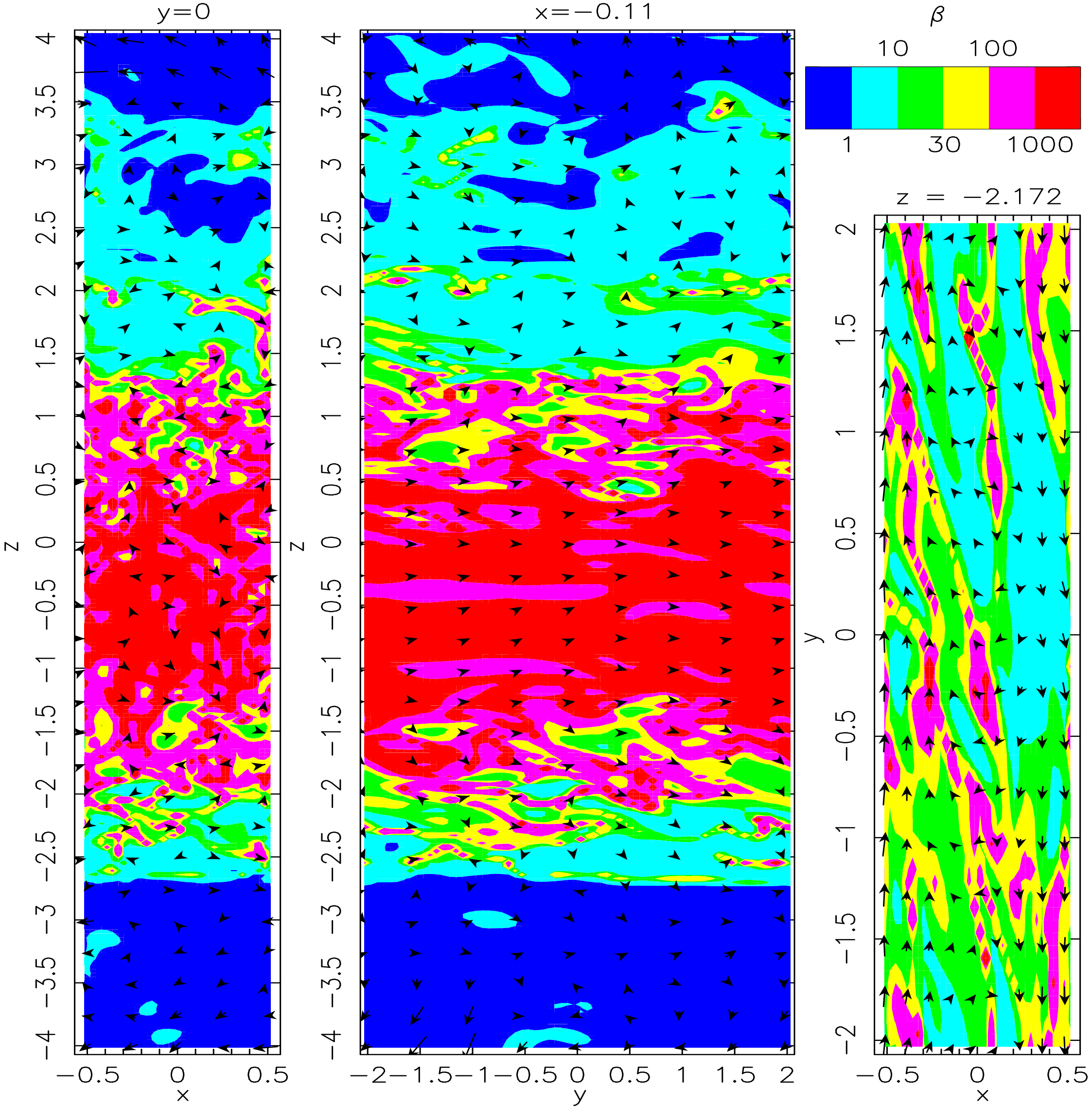

- $\beta = 8\pi\rho c_s^2/B^2$
- Arrows : $\vec{v}$ field

Snapshot Data (t = 210 rot)

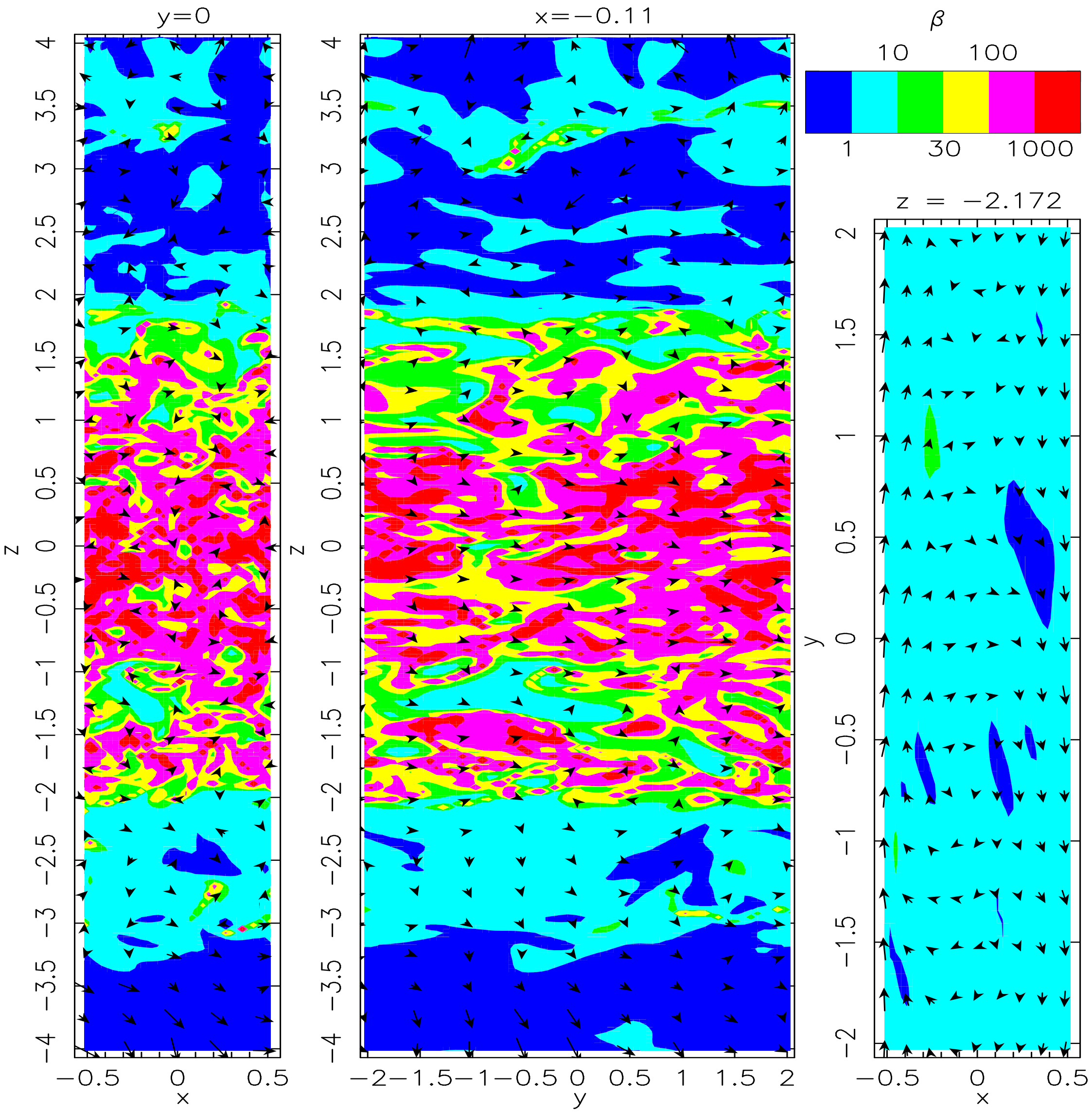

- $\beta = 8\pi\rho c_s^2/B^2$
- Arrows : $\vec{v}$ field

Magnetic Field (t = 210 rot)

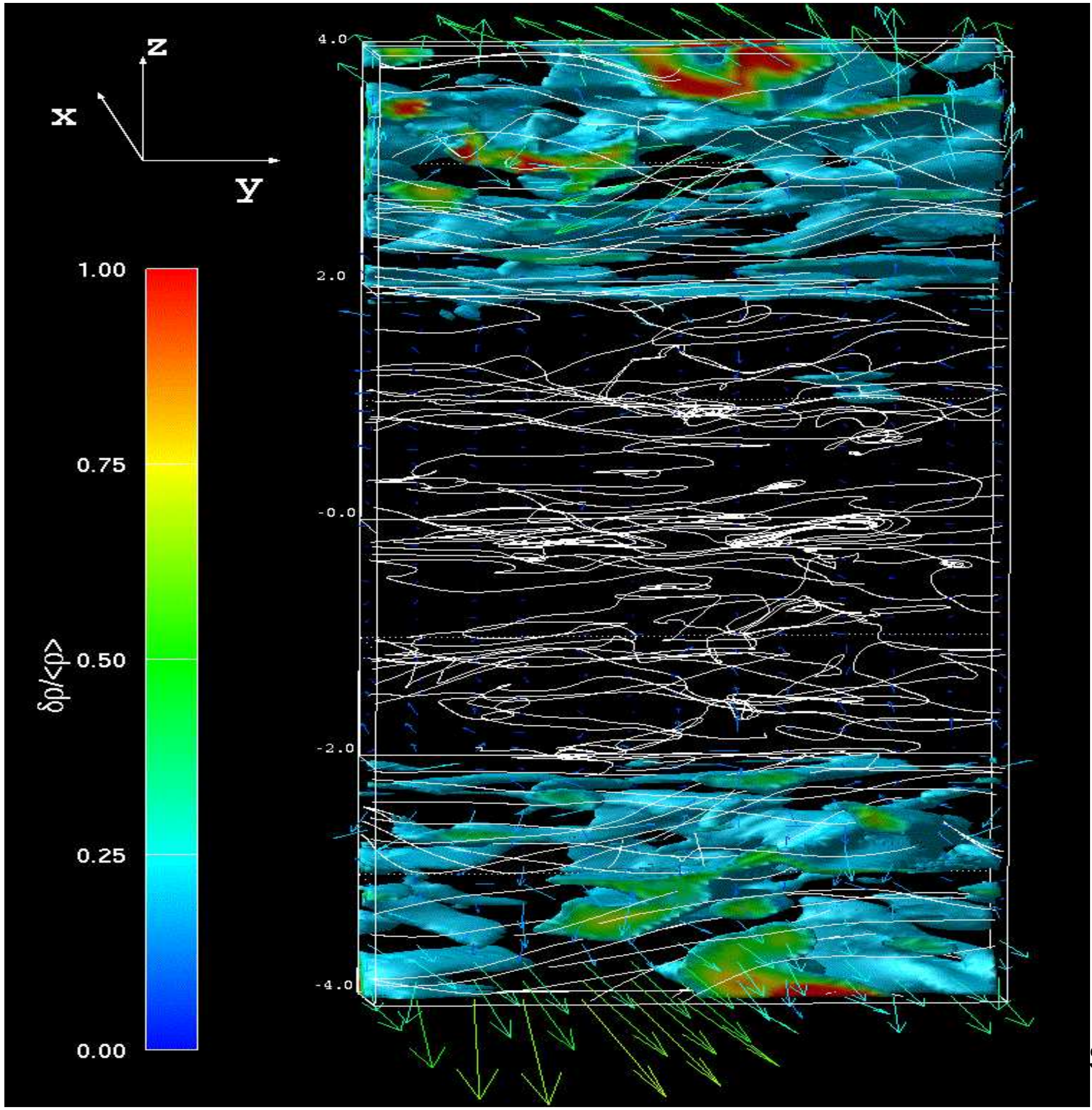

Suzuki & Inutsuka 2009

- Lines:B-field
- Arrows:velocity
- Colors:$\delta\rho/\langle\rho\rangle(>0.2)$

Structure of Disk Winds

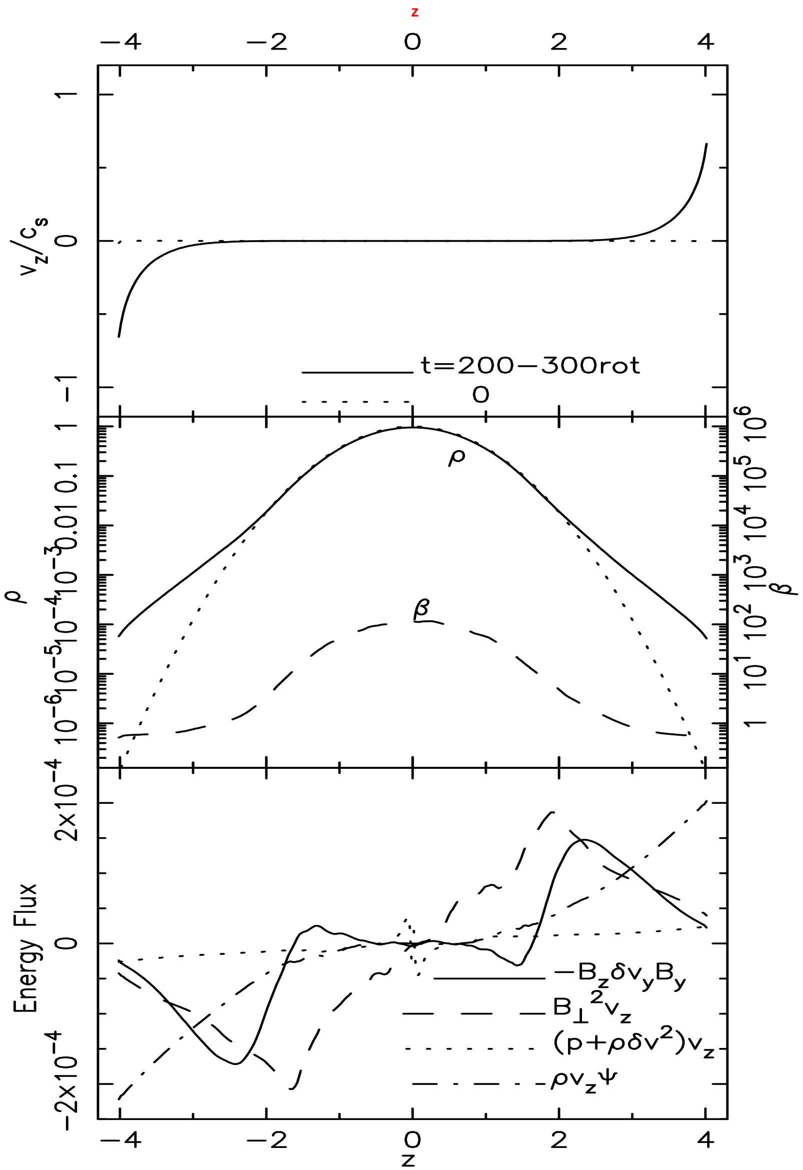

P_mag. >~ P_gas in disk winds

- Winds onset when the magnetic pressure dominates

$$\beta = 8\pi p/B^2 \lesssim 1$$

Disk Winds <= Poynting Flux

- B-Tension ~ B-Pressure

Energy Flux (z-direction):

$$v_z\left(\frac{1}{2}\rho v^2 + \rho\Phi + \frac{\gamma}{\gamma-1}p\right)$$

$$+v_z\frac{B_r^2+B_\phi^2}{4\pi} - \frac{B_z}{4\pi}(v_r B_r + v_\phi B_\phi)$$

where、 $\Phi = z^2\Omega_0^2/2$

Poynting Flux

$\Leftarrow$ **Pressure** & **Tension**

($\Leftrightarrow$ Alfvén waves).

Characterictics of Turbulence

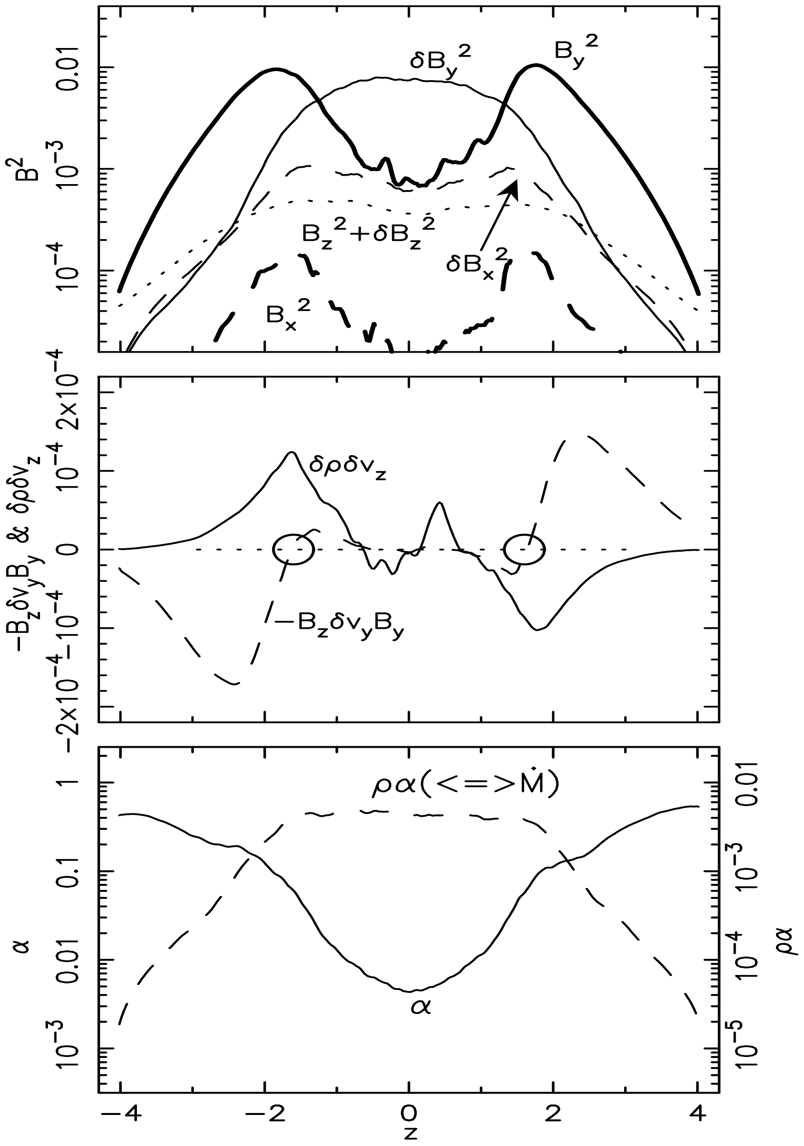

Around z=1.5,-1.5

- **Alfven waves to both directions**
- **Sound waves to midplane**

- Alfvén wave (transverse)
  $w_{\pm} = (v_{\perp} \mp B_{\perp}/\sqrt{4\pi\rho})/2$
  $-B_z v_{\perp} B_{\perp}/4\pi = \rho v_{\rm A}(w_+^2 - w_-^2)$

- Acoustic wave (longitudinal)
  $u_{\pm} = (\delta v_z \pm c_{\rm s}\delta\rho/\rho)/2$
  $\delta\rho\delta v_z = \rho c_{\rm s}(u_+^2 - u_-^2)$

Time-Z diagram of Mass Flux

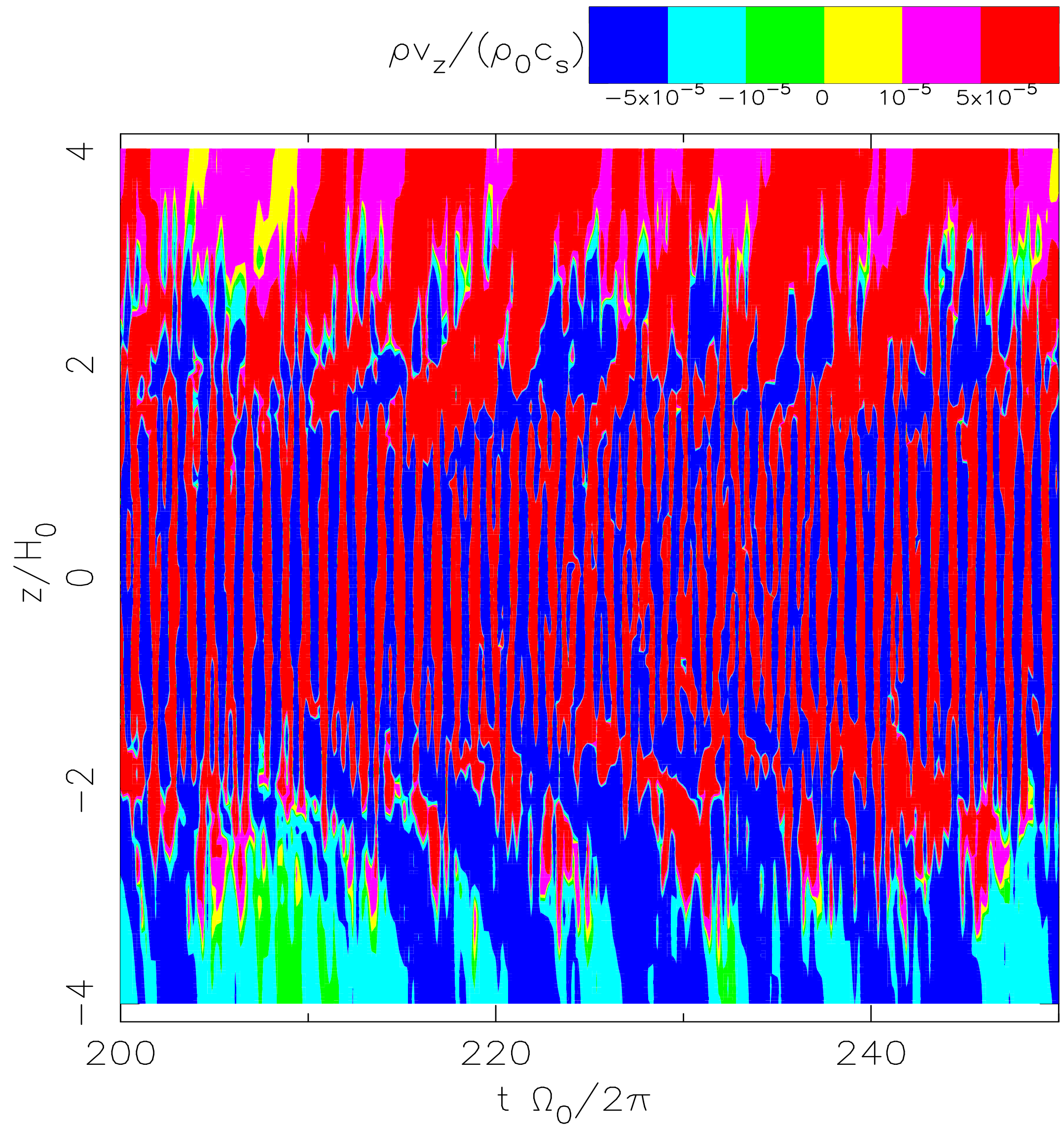

- **Strong winds every 5-10 rotations**
- **Flux to midplane**

Breakups of large-scale channel flows

Characteristics of Turbulence -Schematic view-

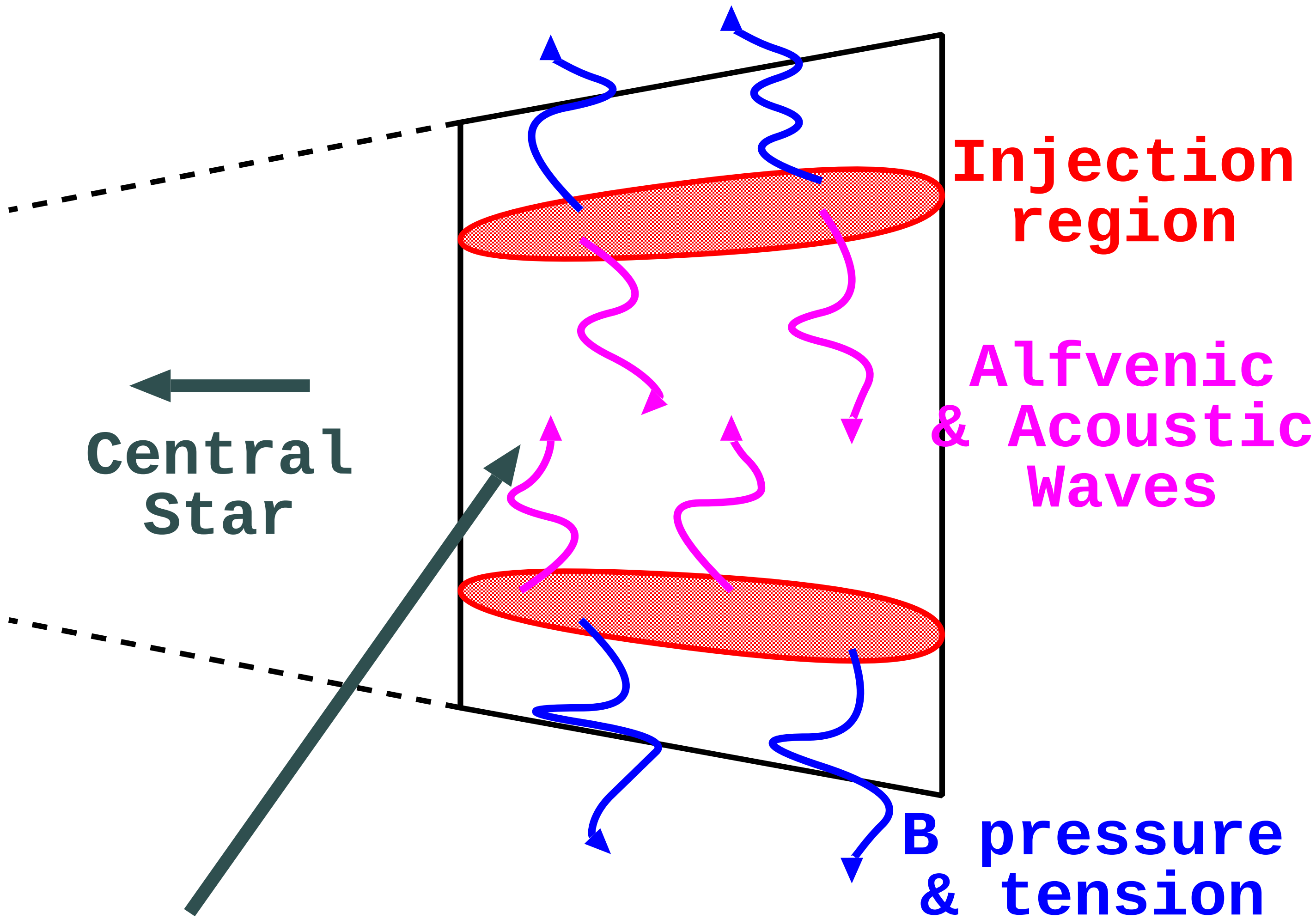

Momentum flux to midplane => Dust sedimentation to midplane

More Local Simulations

Suzuki et al.2009 in preparation

- Dependence on Initial Magnetic Field
- Effects of Dead Zones
- Larger Vertical Box

Dependence on Initial B (1/2)

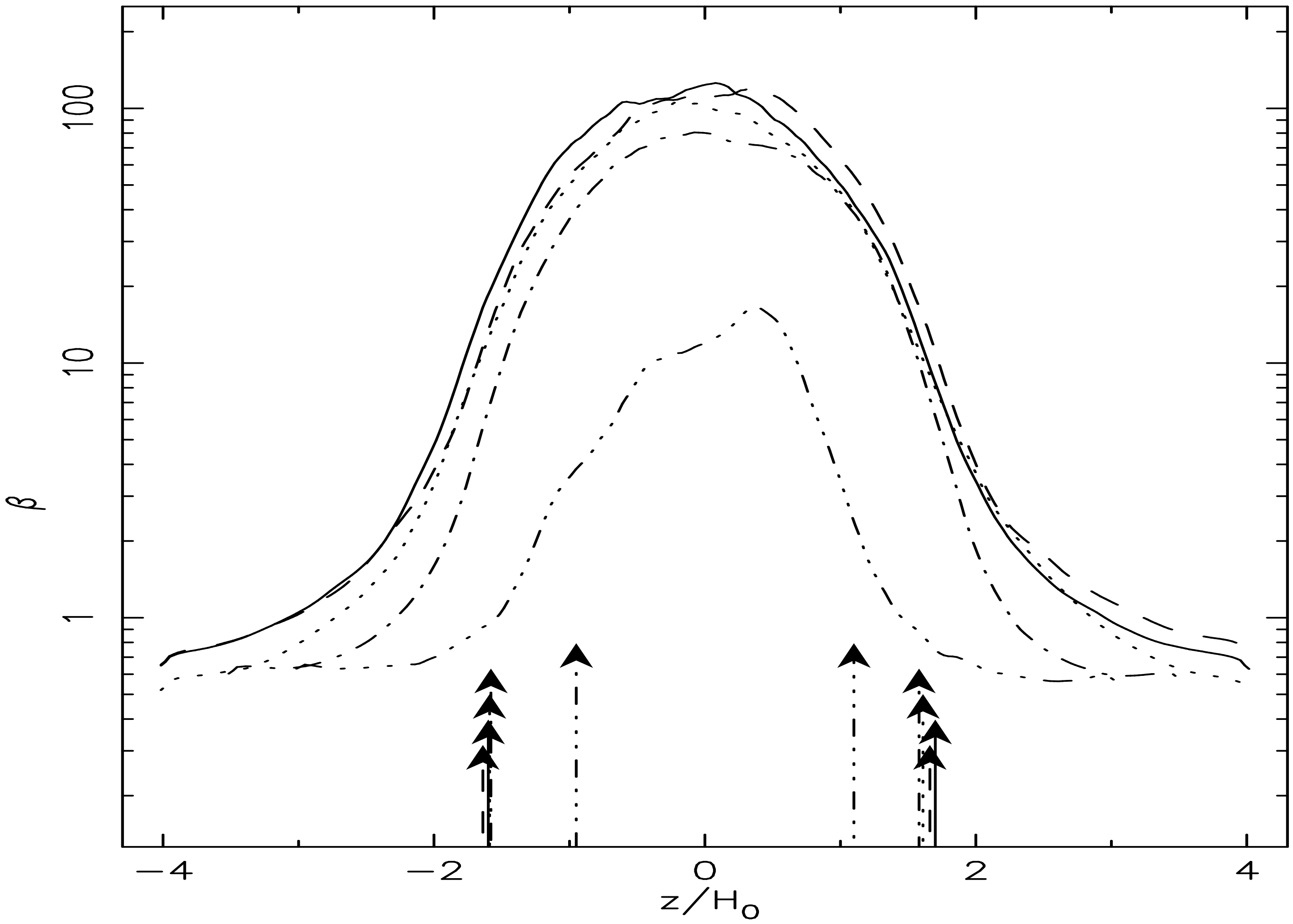

$$\beta_{z,0} = 8\pi p/B_z^2 = 10^4, 10^5, 10^6, 10^7, \infty(\text{only } B_y)$$

$$(\text{Reference case}: \beta = 10^6)$$

Dependence on Initial B (2/2)

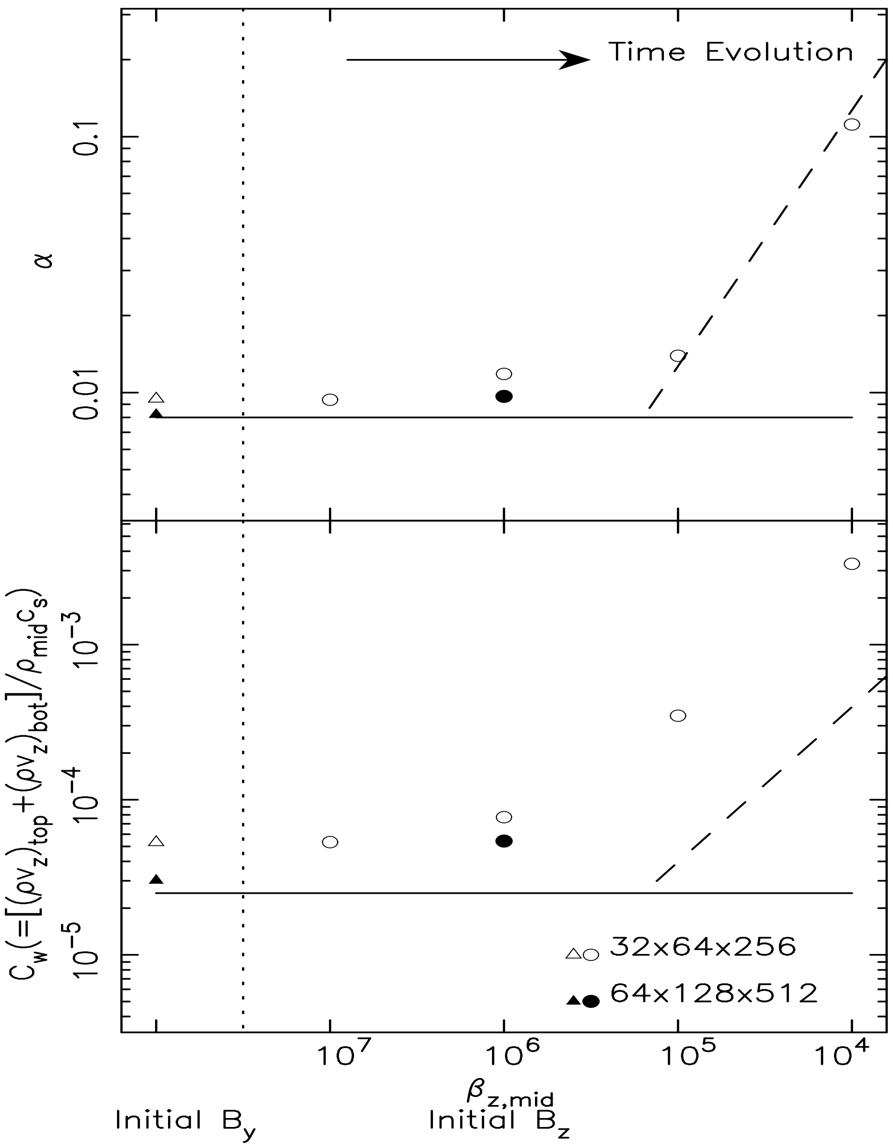

- Weak dependence for $\beta_{z,0} \gtrsim 10^6$
- Higher resolution : smaller α and wind

Effects of Dead Zone

We have assumed ideal MHD (strong coupling between gas and B-field)

- **B-field <=> electrons (Spiral around B-field)**

  <=> (collisions) <=> Neutrals and Ions

But without sufficient ionization the coupling between gas & B-field becomes weak.

- **Required ionization degree = 1e-13 at 1AU of Min.Mass.Sol.Nebula**

  e.g. Inutsuka & Sano (2005)

- **MRI is inactive if the ionization is smaller**

  => Dead Zone around midplane (Gammie 1996)

Simulations with resistivity(1/2)

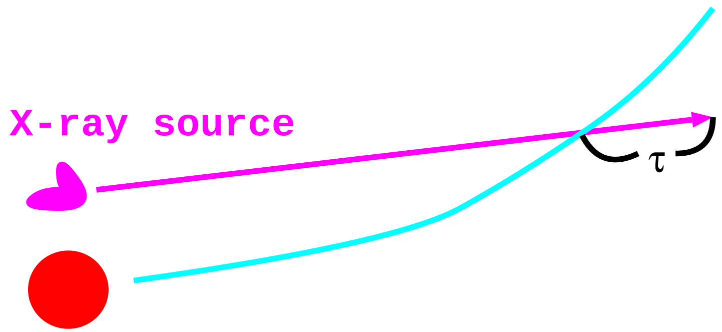

Induction equation :

$$\frac{\partial \boldsymbol{B}}{\partial t} = \nabla \times (\boldsymbol{v} \times \boldsymbol{B} - \eta \nabla \times \boldsymbol{B}) \qquad (\eta \approx 234\sqrt{T}/x_e \mathrm{cm}^2 \mathrm{s}^{-1})$$

Recombination in gas phase : $\mathrm{Mol}^+ + \mathrm{e}^- \longrightarrow \mathrm{Mol}$

where recombination rate, $a = 3 \times 10^{-6}/\sqrt{T}$.

Under steady-state, ionization degree, x_e, is

$$a n_{\mathrm{H}_2} x_e^2 - (\xi_{\mathrm{CR}} + \xi_{\mathrm{X}}) = 0$$

where $\xi_{\mathrm{X}} = \frac{L_{\mathrm{X}}/2}{4\pi r^2 k T_{\mathrm{X}}} \sigma(k T_{\mathrm{X}}) \frac{k T_{\mathrm{X}}}{\Delta \epsilon} J(\tau)$,

Glassgold et al. 1997; Fromang et al.2002

- $\Delta \epsilon \approx 37\mathrm{eV}$
- $\sigma = 8.5 \times 10^{-23} (E/\mathrm{keV})^{-2.81} \mathrm{cm}^2$
- τ is estimated from the following geometry.

Simulations with resistivity(2/2)

Obs. of T-Tauri stars

- **Lx = 1e29 - 1e31erg/s**
- **Ex = 1 - 5keV**

Example : Lx = 1e29erg/s; Ex = 1keV

- **Largest Dead Zone case**

Disk Wind Structure

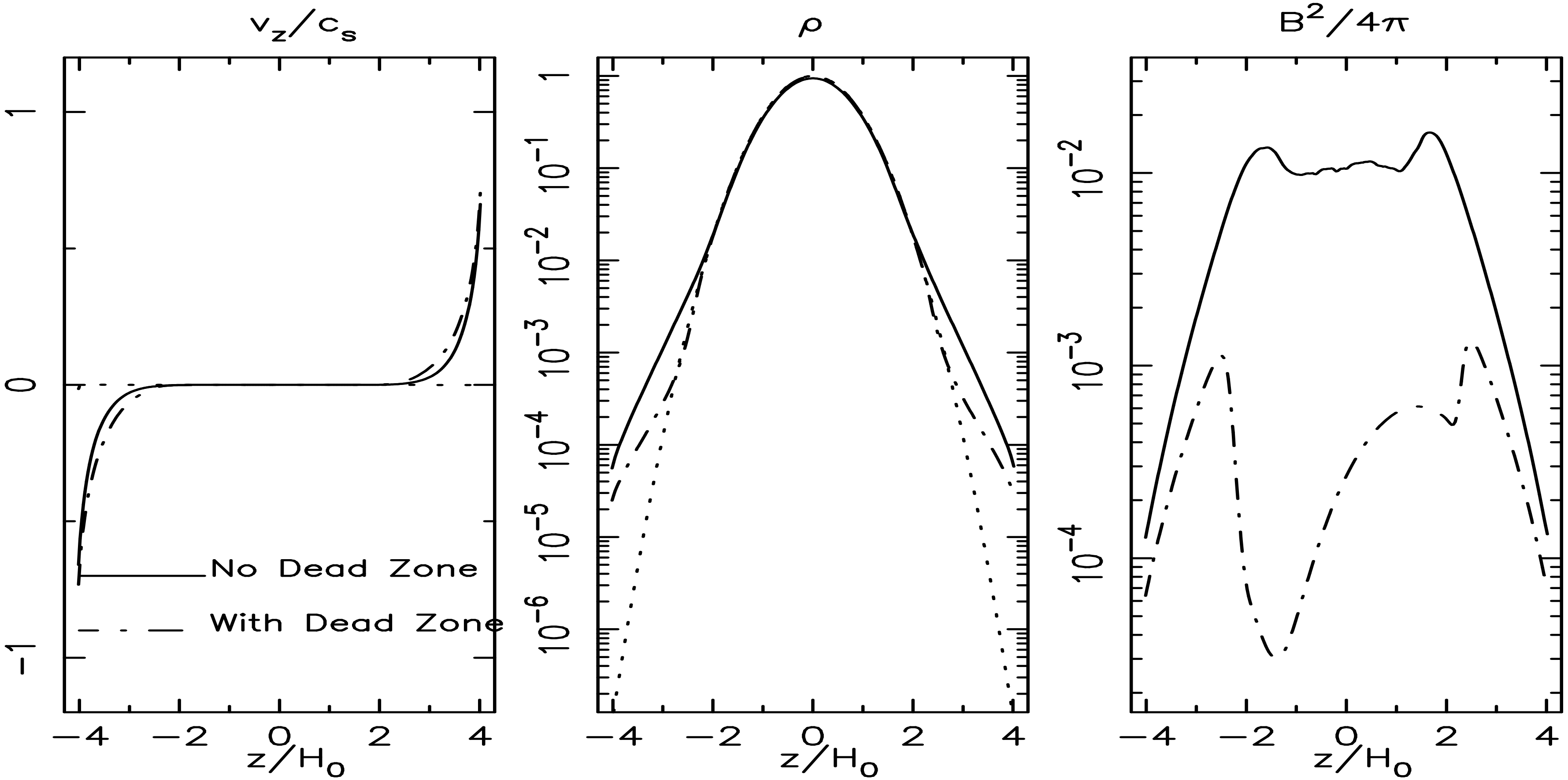

- **No turbulence around midplane**
  - **alpha = 5e-4 (ideal MHD : alpha~1e-2)**
- **Mass flux of disk winds become half.**

Effect of Vertical Box Size

We assume outgoing boundary conditions at the +/- z boundaries.

<= The validity should be tested.

Simulations with larger vertical boxes.

- **Realistic z-gravity.**

$$g_z = \frac{GM_\star z}{(r^2+z^2)^{3/2}} = \Omega_0^2 z \frac{r^3}{(r^2+z^2)^{3/2}}$$

Simulation result -larger vertical box size-

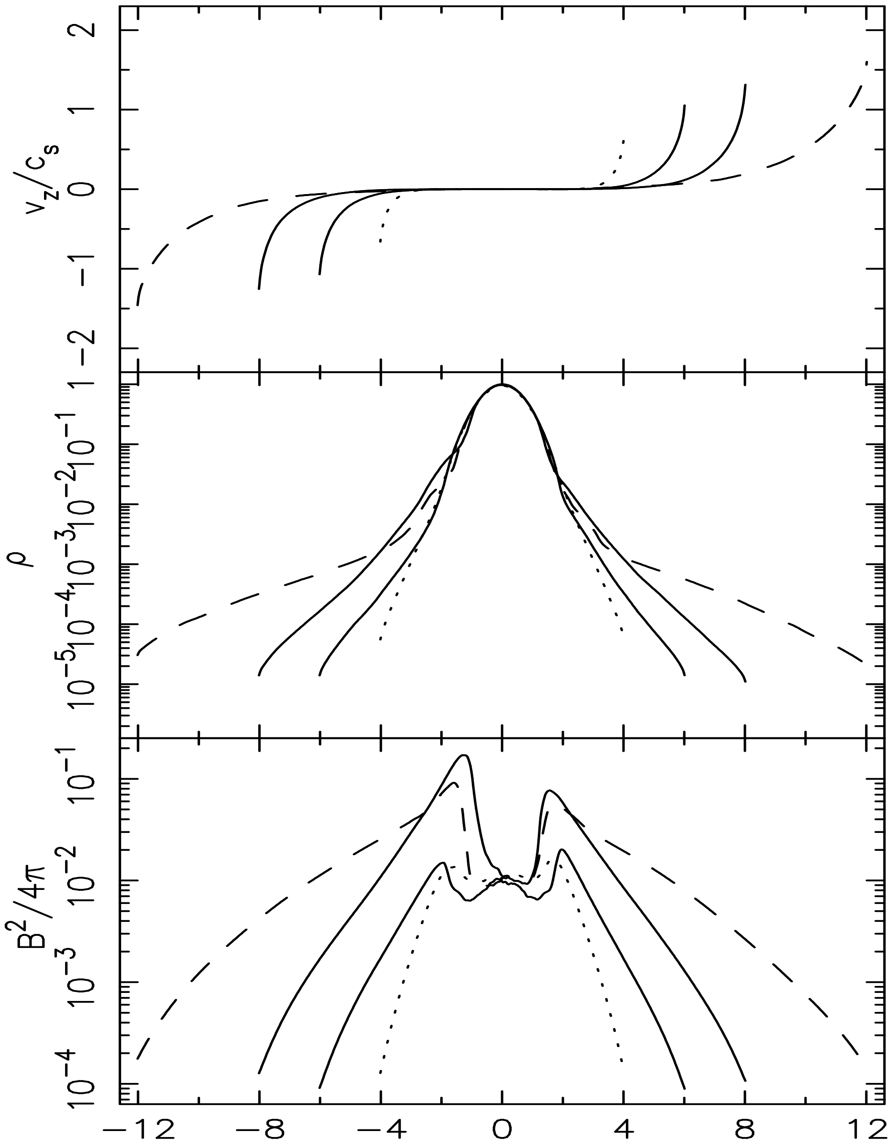

- Dotted : Reference case
- Solid : r=20H
- Dashed : r=10H

- Slower than the escape speeds,

but

- the acceleration continues

Dependence of Disk Wind Mass Flux

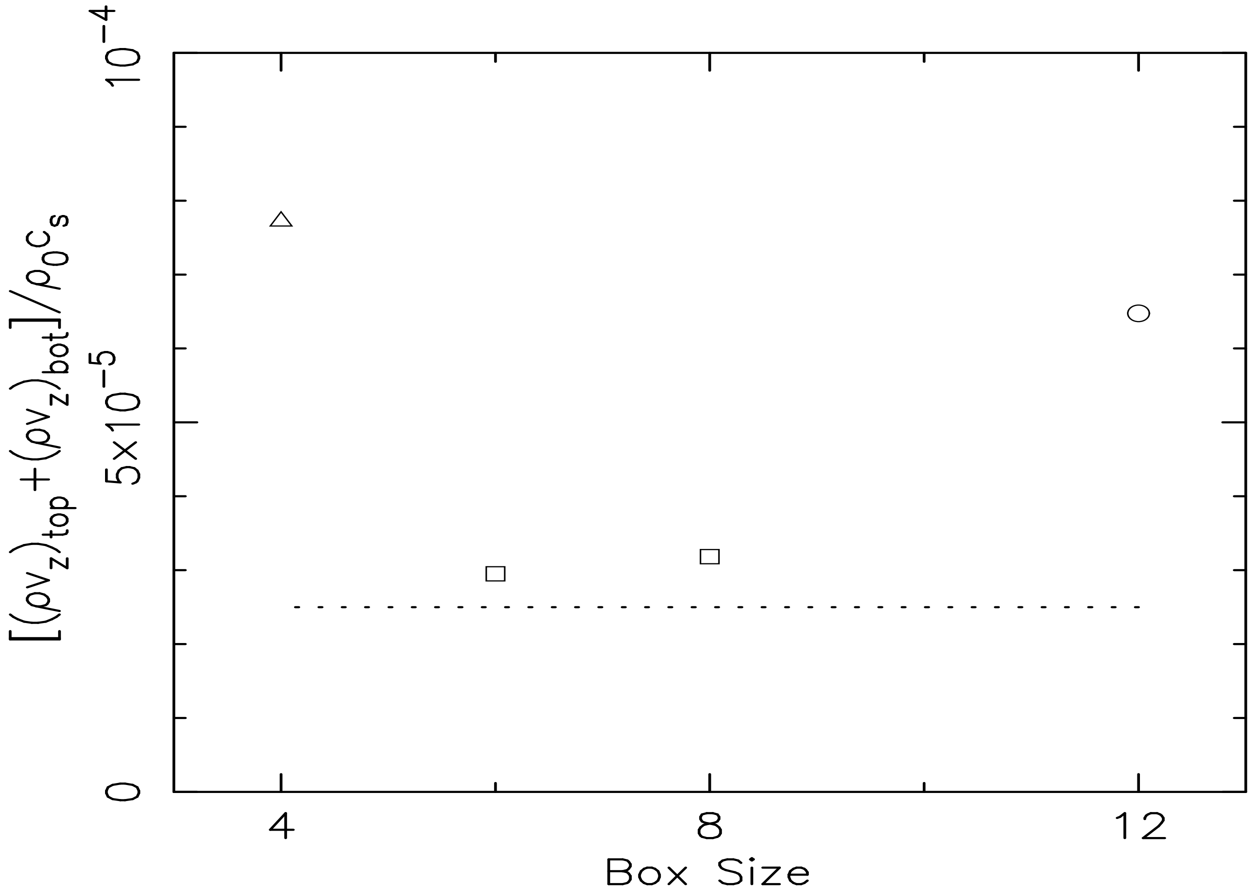

- The mass flux decreases for larger box size, but
- The mass flux seems to have a 'floor value'.

Self-Regulation of Mass Flux

Larger simulation box size

=> The disk wind mass flux decreases

=>The magnetic fields do not escape from the box

- **Toroidal & Radial Magnetic Field**

=> Larger Magnetic Field

=> Larger Magnetic Pressure

=> More gas is lift up

=> Larger Density

=> Mass Flux (density*velocity) increases

2. Global 1D Evolution

1D Calculation

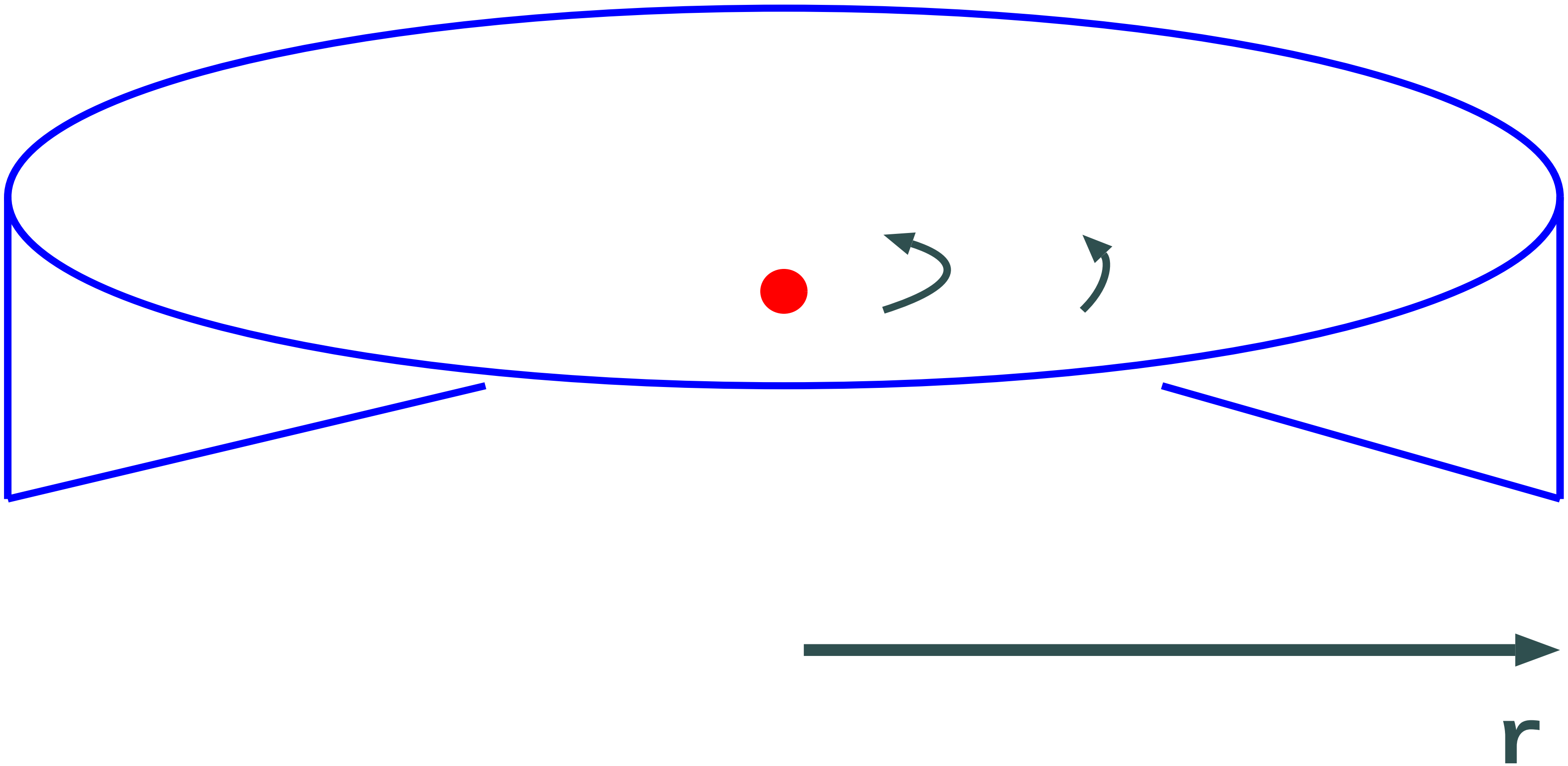

Evolution of Surface Density

$$\frac{\partial \Sigma}{\partial t} - \frac{1}{r}\frac{\partial}{\partial r}\left[\frac{2}{r\Omega}\frac{\partial}{\partial r}(\Sigma r^2 \alpha c_s^2)\right] + (\rho v_z)_{\rm w} = 0 \qquad (1)$$

$\Sigma(=\int \rho z)$ is surface density.

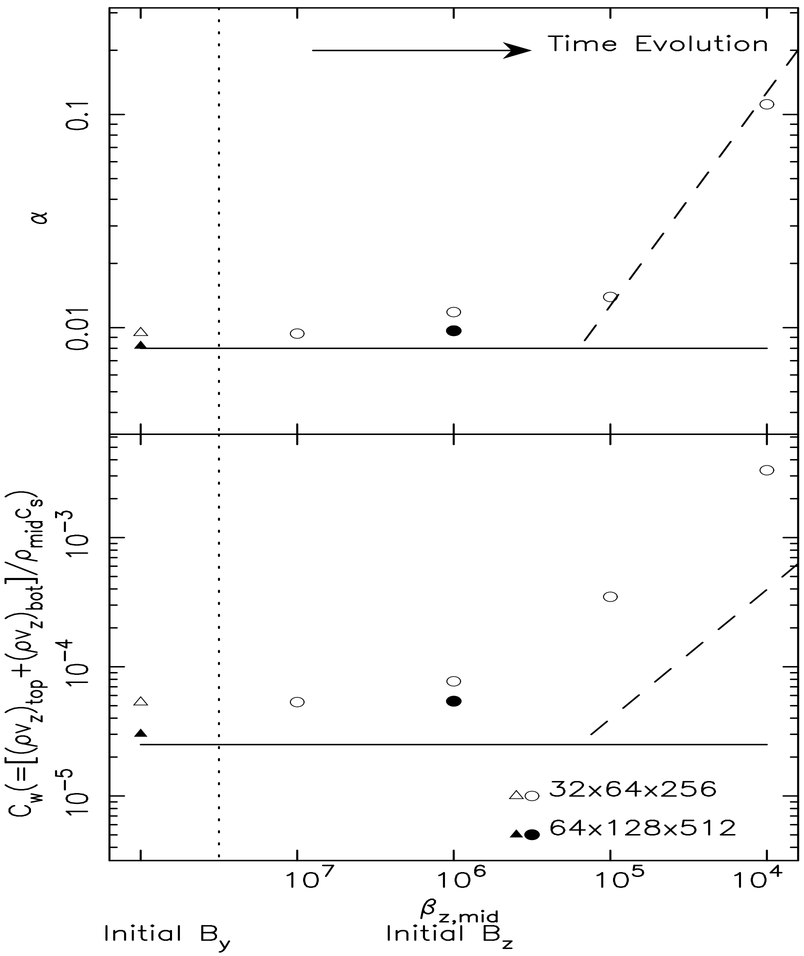

Disk Evolution

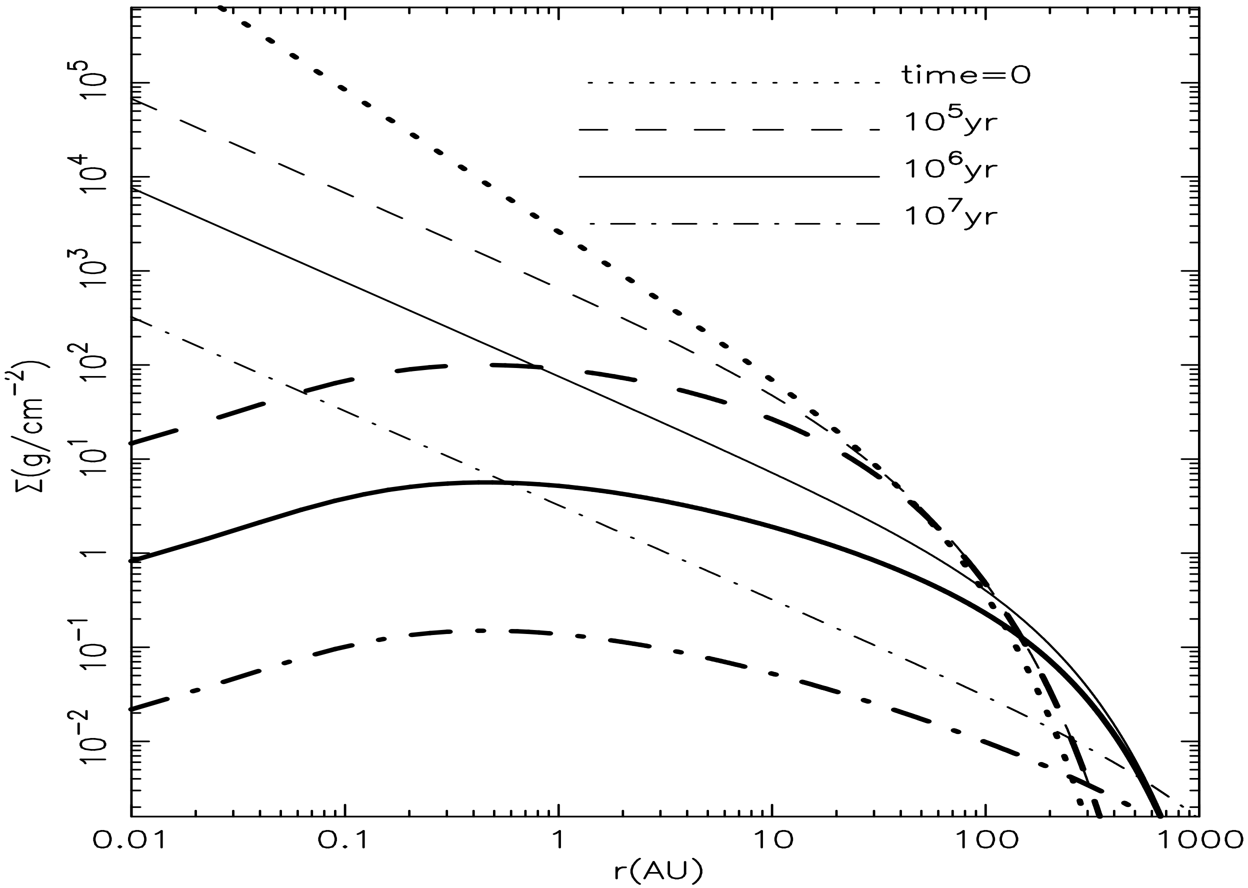

Thick : Disk Winds

Thin : NO Disk Winds

- **Initial condition: Minimum Mass Solar Nebula (Hayashi 1981)**

Explanation of Disk Evolution

No Disk Wind case

Approaching to Self-similar Solution :

$$\Sigma \propto \frac{r_{\rm s}}{r\tilde{t}^{3/2}} \exp\left(-\frac{r}{r_{\rm s}\tilde{t}}\right),$$

$$\text{where } \tilde{t} = \frac{2\alpha c_s^2}{r_{\rm s}} t + 1$$

$$(\text{in } r < r_{\rm s},\ \Sigma \sim r^{-1};\ \text{in } r > r_{\rm s},\ \Sigma \sim \exp(-r/r_{\rm s}\tilde{t})).$$

Disk Wind Case

The Scaling of the disk wind mass flux :

$$(\rho v_z)_{\rm w} = C_{\rm w}\rho_{\rm mid}c_s \propto C_{\rm w}\Sigma\Omega \propto \Sigma r^{-3/2},$$

- **The mass flux is proportional to (Keplerian) rotation frequency.**
- **The mass flux is larger in inner locations. => inner hole of gas disk**

Energetics of Disk Winds

$$\frac{\partial}{\partial t}\left[-\Sigma\frac{r^2\Omega^2}{2}\right] + \frac{1}{r}\frac{\partial}{\partial r}\left[r\Omega\frac{\partial}{\partial r}(r^2\Sigma\alpha c_s^2) + r^2\Sigma\Omega\alpha c_s^2\right] = Q_{\rm loss},$$

$Q_{\rm loss} \Leftarrow$ (Wind) + (Cooling) - (Heating) ; We neglect cooling/heating.

If $\frac{\partial}{\partial t}\left[-\Sigma\frac{r^2\Omega^2}{2}\right] + \frac{1}{r}\frac{\partial}{\partial r}\left[r\Omega\frac{\partial}{\partial r}(r^2\Sigma\alpha c_s^2) + r^2\Sigma\Omega\alpha c_s^2\right] - \frac{3}{2}\rho v_z r^2\Omega^2 \leq 0$
is satisfied, the disk winds are potentially accelerated to infinity.

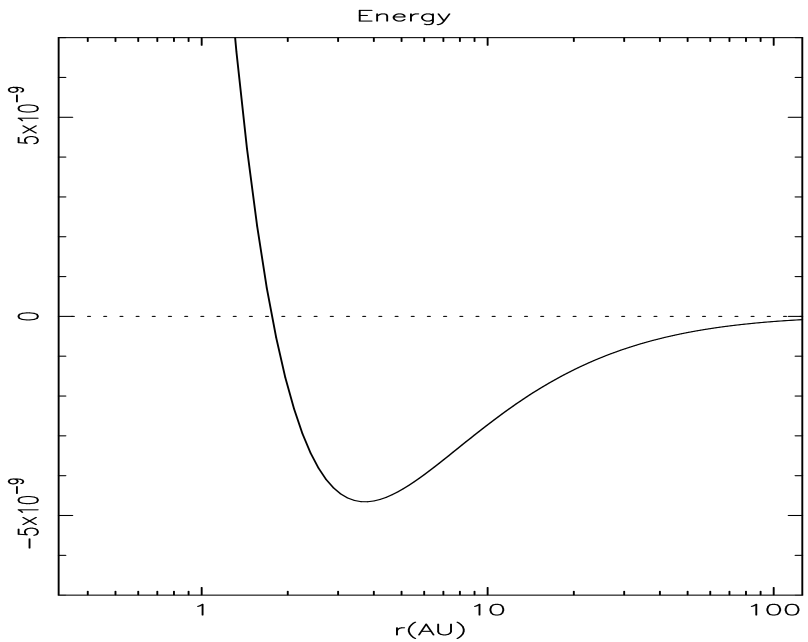

- **Sufficient energy in r > 1.7AU**

Summary

Disk Winds driven by MRI trigerred turbulence

- **(Grav. E.=>)Mag. E.=> Disk Winds**
- **Wind onsets when Mag.E > Gas E.**
- **Initially Toroidal & weak vertical field cases give similar structure**
- **Dead zones reduce the mass flux slightly (~half).**
  - **alpha value is reduced to ~1/(10-100)**
- **The wind strucure depends on the vertical box size, but the wind mass flux is not so affected much.**

Global Evolution

- **Gas dissipates from inner regions by disk winds.**